

Synthesis and Fabrication of In_2O_3 : CdO Nanoparticles for NO_2 Gas Sensor

Ashwaq T. Dahham^{1*}

Kadhim A. Aadim²

Nada K. Abbas¹

Received 25/4/2018, Accepted 15/7/2018, Published 13/9/2018



This work is licensed under a [Creative Commons Attribution 4.0 International License](https://creativecommons.org/licenses/by/4.0/).

Abstract:

The physical and morphological characteristics of porous silicon (PS) synthesized via gas sensor was assessed by electrochemical etching for a Si wafer in diluted HF acid in water (1:4) at different etching times and different currents. The morphology for PS wafers by AFM show that the average pore diameter varies from 48.63 to 72.54 nm with increasing etching time from 5 to 15min and from 72.54 to 51.37nm with increasing current from 10 to 30 mA.

From the study, it was found that the gas sensitivity of In_2O_3 : CdO semiconductor, against NO_2 gas, directly correlated to the nanoparticles size, and its sensitivity increases with increasing operating temperature.

Keywords: AFM, Gas Sensor, Metal Oxide Semiconductor, Porous Silicon.

Introduction:

The possibility of changing some of semiconductor materials properties (such as electrical and structural properties) by doping, making a mixture of them or making them in nanosized shapes has made them very important in many an application of general rules to particular cases such as in solar cells (1, 2), optoelectronics (3-5), spintronic (6), piezoelectric and gas sensors (7-8). There have also been studies showing that when semiconductors are exposed to some gases, lead to change their electrical properties. This phenomenon is used in the application of gas sensing (9-11). The sensitivity of semiconductor against target gas can be improved by doping or making composite (12-15) or by reducing their particles to nanosized (16, 17) or by increasing operating temperature. Porous silicon (PSi) having distinctive physical and chemical properties which differ from single crystal Si properties. Some of these properties are significant in gas sensor technology field. In the PSi some part silicon crystals etched away by the electrochemical process make the silicon surface contains many pores. As a result, numerous and unusual physical phenomena can be observed (12, 13).

Cadmium oxide is an n-type semiconductor, crystal structure (FCC) with direct optical energy gap (4).

¹ Department of Physics, College of Science for Women, University of Baghdad, Baghdad, Iraq

² Department of Physics, College of Science, University of Baghdad, Baghdad, Iraq

*Corresponding author: ashwaqtariq@yahoo.com

Its electrical accessibility is rise, also the ratio of light energy falling on a body to transmitted through it, in the visible region makes it helpful for different applications, photodiodes, gas sensors, etc. (5).

Indium oxide is a wide band gap n-type semiconductor with direct band gaps of 3.75 eV, with a cubic bixbyite structure. It is a best material used as in transparent conducting oxide (18).

Operating temperature is an essential parameter for gas sensitivity. Also, the crystallinity is an important thing that alter semiconductor electronic properties which is the basic for gas sensitivity. Gas sensors depend on CdO semiconductors against different gases have been widely reported (8).

Porous silicon (PS) for a crystalline silicon, having within it a branch of nano-sized pores, it has a direct wide energy gap and high resistivity. The most important advantage of PS is the layers and its great and interacting internal surface. That the internal surface would play a significant role in the specific properties of PS layers enabling this material to be entirely different from the bulk (9). Electrochemical etching is a more applied technicality for the synthesis of PS (10).

In this study, the morphology, nanoparticle size of PS and properties gas sensing using a static gas sensing system were examined. Nanostructured of In_2O_3 : CdO films have been tested that several gases. These were observed to be more selective than NO_2 at different operating temperatures. There was a robust connection between the surface and the bulk in semiconductors, illustrate why these

materials are used as gas sensors in addition to many other applications. The practical form of appearance of semiconductor gas sensors is different for a thin film with a comparable thickness of the space charge layer to the total layer thickness (simple, or with the doped surface) (14, 15). The sensing mechanism is based on changes in the film's resistance, which is controlled by gas species. The sensitivity (S) of the film is defined as the ratio of the film resistance in air (R_{air}) and gas (R_{gas}). Mixed semiconductor was used in many researches to detect different gases at a relatively low operating temperature (16 - 18). Must be used synthetic approaches or used subsequent analytical size selected methods to controlled the morphologies and dimensions of Silicon nanoparticles (19). This study investigates the effect of morphological characteristics of porous silicon on In_2O_3 : CdO nanoparticles as a gas sensor.

Material and Method:

In_2O_3 : CdO thin films for In_2O_3 doped with 0.09 wt.% CdO were synthesised using a technique pulsed laser deposition technique using Nd: YAG laser. The thin films were grown in a vacuum chamber with a background pressure of $\sim 1 \times 10^{-3}$ mbar. The Nd: YAG laser has a wavelength of $\lambda = 1064$ nm with 6 Hz frequency. Morphologically characteristics of the porous silicon (PSi) structure were fabricated using an electrochemical etching process in HF acid. In_2O_3 : CdO/Psi was produced via the deposition of In_2O_3 : CdO. Electrochemical etching formed the PS. F^- ions are previously obtained available in sufficient amounts at the surface which agrees with (20).

Heater consists of a hot plate and a K-type thermocouple located inside the chamber to control the operating temperature of the sensor, and a bias voltage between the two sides of the electrode is applied. A switch on the rotary pump clears the test chamber for approximately 1 mbar, and the gas sensor is set to the desired operating temperature. where in the gas is tested under a different volumetric concentration of gas to air ratio, Resistance variation is measured using a computer connect to a digital multimeter. Initially, the biasing air flow resistance records by the digital multimeter records. After turning on the multimeter for several seconds, the testing gas (NO_2) shows a low variation of resistance. After switching off the device, the test gas is used to record the recovery time to give the real sensitivity corresponding to Ali Ahmad Yousif, (21). The sensitivity is calculated by applying Equation (1), as given in (22):

$$S = \frac{|R_g - R_a|}{|NR_a|} \times 100 \% \dots (1)$$

where (R_a) and (R_g) represent the electrical resistance of the sensor in air, and the presence of gas respectively and (N) is the gas concentration. This may also be calculated from conductance as in Equation (2), (23):

$$S = \frac{\sigma_g}{\sigma_a} \dots (2)$$

σ_g is the film conductivity in gas, while σ_a is represented the film conductivity in air under $300^\circ C$.

A layer of porous silicon is doped with In_2O_3 , with a CdO ratio concentration of 9 wt.% of wafer silicon (P-type) and with an orientation of 100, resistivity 0.01 - 0.02 and a thickness of $525 \pm 25 \mu A$. The PS samples were prepared by the electrochemical etching (ECE) method in hydrofluoric (HF) acid 17 %, and the concentration and the etching cell are made from Teflon as this does not act in such a way as to have an effect on another with HF acid, and a rubber O-ring is used before the up part of the cell. The electrochemical cell used has two electrode configurations with a platinum (stainless steel) and electrode as a cathode, and a silicon wafer as an anode. Platinum is one of the least reactive metals. It has remarkable resistance to corrosion, even at high temperatures, and is therefore considered a noble metal. Consequently, platinum is often found chemically uncombined as native platinum. Because it occurs naturally in the alluvial sands of various rivers, Platinum is used in catalytic converters, laboratory equipment, electrical contacts and electrodes, platinum resistance thermometers, dentistry equipment, and jewelry. Being a heavy metal, it leads to health problems upon exposure to its salts; but due to its corrosion resistance, metallic platinum has not been linked to adverse health effects (24). A digital millimetre device was connected to the silicon, and the other side was connected to the power supply. After cutting the silicon samples into $2.25 \times 2.25 \text{ cm}^2$ pieces, washes the wafer is with acetone and methanol to eject any oxide layer. The samples were put in 48 % concentration of acid in a mixing ratio 4:1 HF.

Using chemical ethanol with a purity of 99.9 % and a concentration of 17 %, different etching times of 5, 10, 15 min, at a constant current of 20 mA, and with various currents of 10, 20, 30 mA was applied. Applying a constant etching time of 30 min for the development time, plus the addition of the mixing motor, helped the electrical conduction process. This led to the acceleration of the emptying of bubbled hydrogen (H_2) as a catalyst and alcohol ethanol that was used for the evacuation process. The porous silicon samples were next washed in ethanol after their removal from the

solution. The samples were left to dry at ambient temperature for several minutes and then stored in containers put within including methanol to stop the formation of an oxide layer on the prepared samples.

Results and Discussion:

Atomic force microscopy (AFM):

Atomic force microscope (AFM) was used to obtain microscopic facts provided of the surface structure and fraction the topographies of the surface comfort. Figure 1 and Figure 2 show the (AFM) of the surface morphology of the oxidised PS layer. This focused completely on the size measurable in nanometres characteristics of the pores silicon films when the etching time increased. Fraction of the pores coagulated to form big structures corresponding to (25), showing AFM images of the porous silicon for both cases. Distributed nanocrystalline silicon pillars randomly and space on top of the all surface could be observed. Pore morphology resulted when the current flowed in the electrochemical cell. The dissociation reaction was localised on the distinct side of the silicon surface, thus initiating the etching

of an array of the pores in the silicon wafer. At the high etching time, a highly branched, randomly directed and highly interconnected mesh-work of the pores was obtained. AFM parameters (average diameter and roughness) for these samples are shown in Table 1. Several affecting parameters were examined such as the current density and etching time. Morphological property (AFM) parameters were examined for porous silicon wafer at a constant current of 20 mA for different etching times of 5, 10, 15 min respectively. An average diameter of porosity and that the PS layer thickness increased with increasing etching time. Furthermore, the average diameter pore range was observed between 48.63 - 72.54 nm, and with various currents of 10, 20, 30 mA the average diameter of porosity and thickness of the PS layer showed decrease with increasing the current density at constant etching time of 30 min. An average diameter pore range between 72.54 -51.37 nm. The pore width was classified as mesoporous type, as shown in Table 2, which corresponds to the results found by Patil et.al. (22). and this in agreement with the results found by Biswas et.al. (26).

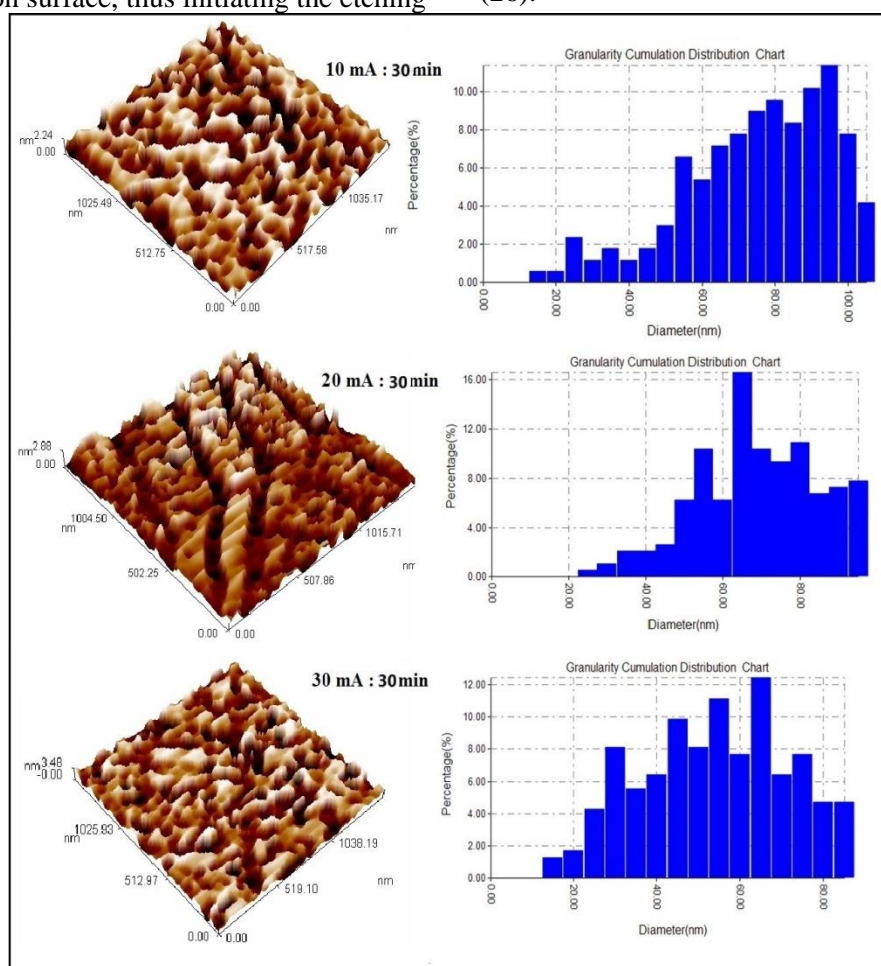


Figure 1. Atomic Force Microscopy (AFM) of porous silicon at different currents, 10, 20 and 30 mA at constant etching time of 30 min.

Table 1. Atomic Force Microscopy (AFM) of porous silicon at different currents, 10, 20 and 30 mA at constant etching time of 30 min.

Current (mA)	Ave. diameter (nm)	Roughness average (nm)	Root mean square (nm)
10	72.54	0.581	0.665
20	66.35	0.632	0.741
30	51.37	0.862	0.995

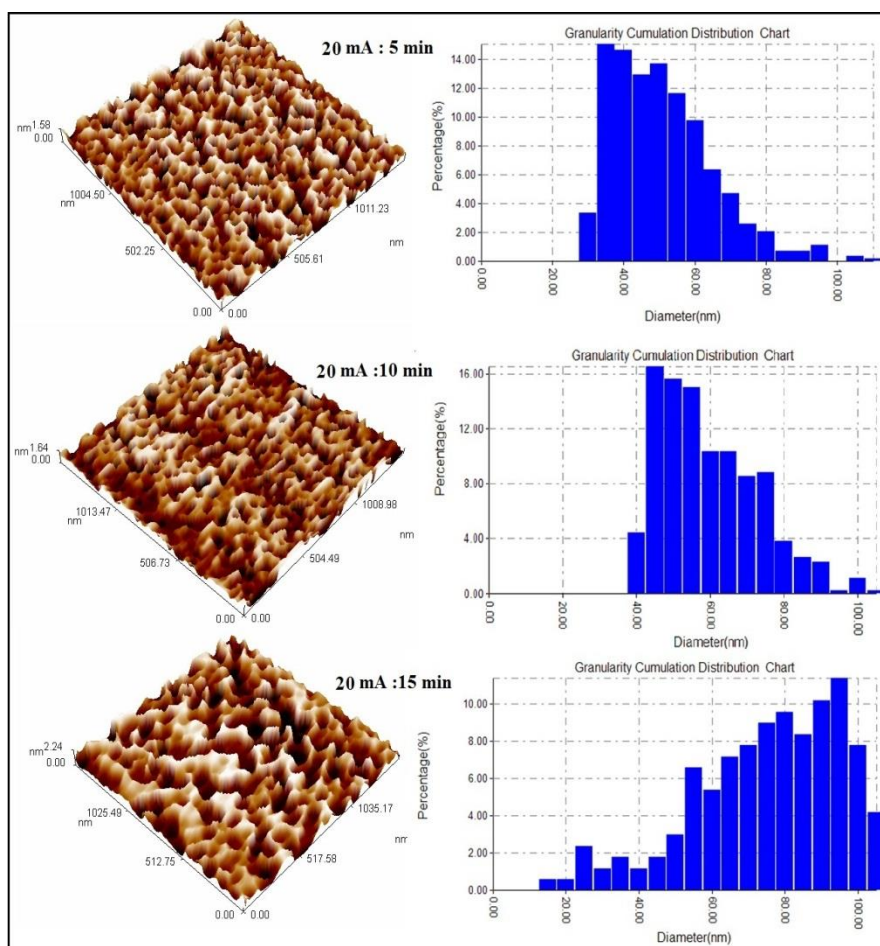


Figure 2: Atomic Force Microscopy (AFM) of porous silicon at different etching times, 5, 10 and 15 min at constant current of 20 mA.

Table 2. Atomic Force Microscopy (AFM) of porous silicon at different etching times, 5, 10 and 15 min at constant current of 20 mA.

time (min)	Ave. diameter (nm)	Roughness average (nm)	Root mean square (nm)
5	48.63	0.402	0.464
10	57.55	0.386	0.445
15	72.54	0.581	0.665

Gas sensor:

Principle.

The increase or decrease of the semiconductor sample resistance, when exposed to target gas, depends on the type of majority carriers and the nature of gas molecules (whether oxidising or reducing) at the surrounding. The resistance of the thin film was increase when the materials were n type, oxidising gases acceptor while reducing gases (donor) decrease with correspondingly for p-type materials (27).

The transfer of electrons during the adsorption and desorption of gas molecules because of the chemo

resistance of the metal oxides which is responsible for the width of the depleted region formed on the crystallites. The offer of the space charge region acts as a potential hurdle in the conduction system operation between the grains, succeed in persuading changes over time in the Fermi level. due to the depletion of electrons, the band bends upward When the oxidising gas interacted with the n-type material and due to the accumulation of electrons for the reducing gas, the band bends downwards (28).

The operating temperature effects sample sensitivity through its effect on the chemical dynamics between gas-solid and thus limits the sensor properties such as sensitivity, selectivity, stability, response and recovery times (29). Also, the humidity level has a much higher influence on the sensor response (30), due to the variation in electronic and ionic conducting properties of the semiconducting metal oxides when adsorbed water vapour on its surface.

Oxidation mechanisms for oxidising gas molecules

Oxygen (O₂)

Oxygen is one of the most important oxidizing gases, which quickly adsorbs the surfaces of metal oxides. This adsorption can be enhanced by increasing operating temperature, using vaccination and reducing grains size (25). O₂ can accept one electron, when the temperature below of 200 °C, and it can accept two electrons from the metal oxide surface when the temperature above 200 °C, (31, 32). When The adsorbed oxygen molecules/atoms are interacting with other gas molecules, they are desorbed quickly

(NO₂) Nitrogen Dioxide

NO₂ is a potent oxidising factor and has a robust electrophilic advantage (33), which enables the molecule to become rapidly adsorbed on the metal oxide surface. Nitrogen dioxide ability interact together a surface in the appearance and non-attendance from O₂ (34). The oxidation of NO₂ leads to the reduction of conduction electrons in the conduction band. Nitrogen oxides are among the six most common air pollutants. Nitrogen gas plays an important role in the production of ozone. For the accuracy of the NO₂ gas sensor has an important role in monitoring emissions processes (35).

To determination the operating temperature of the sensor is presented next. Significant impediment of metal oxide gas sensors is the elevated temperature in demand for sensor operation (30 – 300 °C). For this reason, the effect of the operation temperature of thin films sensitivity is intended with the purpose of optimising the operating temperature to the less than average height from the top possible value and that agree with (16). The sensitiveness semiconductor sensor is specified by the interaction design among the target gas and the sensor surface. The higher surface area of the materials, the robust interaction between the adsorbed gases and the sensor surface, i.e. the higher sensitivity to target gas. The consequence display that the rising in the operating temperature improve the film sensitivity, Such is referring to the increasing rate of surface reactivity of the target gas. The extreme top amount is observed in a confirmed temperature, (optimal temperature) which thereafter decrease, where under other conditions would increase. This expound wherefore the connexion between temperature and sensitivity simulate a hill track for the metal oxide gas sensors (19) and observing the growing and decreases in the sensitivity thereby indicator the adsorption and desorption a fact or situation that is observed to exist of the gases. Figure 3 shows that the value of the resistance increases, when the films are exposed to Nitrogen Dioxide gas, (Gas open), then the resistance value decreases at the shutdown of the (Gas OFF). The cause for this behaviour can be refer, Nitrogen dioxide gas submit an ionic rebuttal with adsorption of oxygen, where the electron is taken away from the semiconductor and causes reduce the conductivity of the materials, thereby increasing the resistance, and that agree with (32).

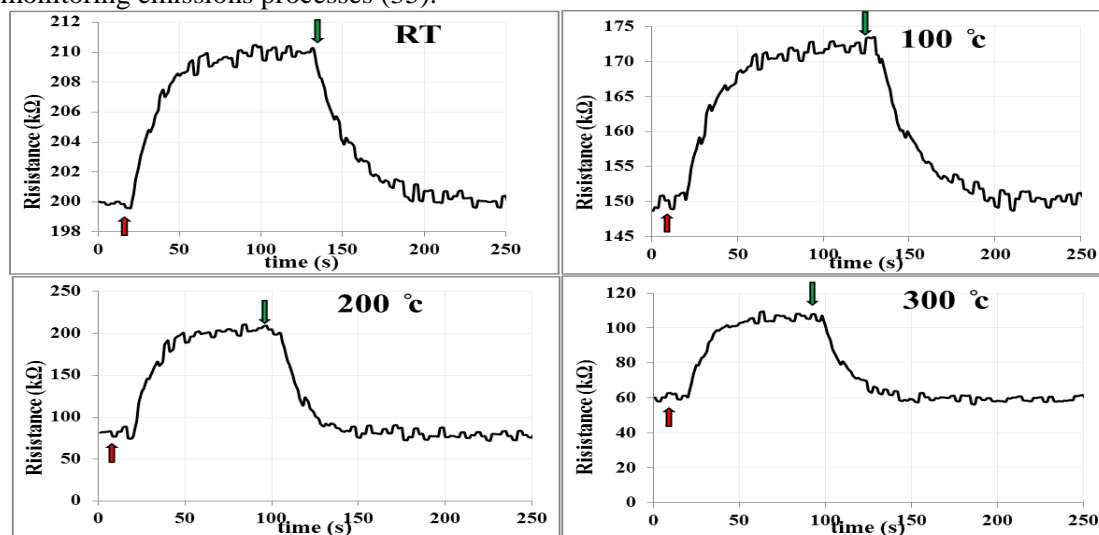


Figure 3. The variable resistance with time for Operating temp for In₂O₃: CdO of porous silicon for NO₂ gas at (a: RT, b: 100 °C, c: 200 °C, d: 300 °C) and etching time of 30 min.

The sensitiveness was seen to excess with the operative temperature up to 100 °C, probably impute to the most favourable conditions rate of oxidation of Nitrogen dioxide (16). The sensitiveness of the In₂O₃: CdO to Nitrogen dioxide was to be 156 % at 200 °C on the silicon substrate which then decreases with additional rise in the operating temperature at an etching time of 30 min. This is agreeing with the result found by Yousif et.al. (21) for, In₂O₃: CdO, films exposed to NO₂ gas which is found that the maximum sensitivity was 142.1 % at concentration of 1 % In₂O₃.

Response Time and Recovery Time

This section describes the relationship between the response time and the recovery time with operating temperature at different etching times, for In₂O₃ doped with 9 % CdO deposited on a porous silicon wafer for 3 % NO₂ mixed with air at a bias voltage of 6 V.

The response \ recovery time is shown as a function of the operating temperature for In₂O₃: CdO and reveals the decrease of response \ recovery time with increasing operating temperature. Table 2 shows that the 30-min etching time sample exhibits a fast response speed of 50 s and recovery time of 75 s at an RT operation temperature. This revealed that a 30-min etching time is an optimal time to achieve a fast response sensor showing the decrease of response and recovery time with increasing operating temperature (21).

Table 3. The difference of sensitivity with operating temperature and the variance of response time and recovery time with operating temperature for In₂O₃: CdO of porous silicon for a NO₂ gas etching time of 30 min.

Operating temp (°C)	Sensitivity (%)	Response time (s)	Recover time (s)
30	5.0	50.0	75.0
100	14.7	60.0	70.0
200	156.0	35.0	40.0
300	78.4	39.0	49.0

Conclusion:

In₂O₃: CdO nanomaterials were prepared using pulsed laser deposition on silicon (100) and porous silicon substrate samples prepared by the electrochemical etching (ECE) method in HF acid at room temperature. The nanoscale improved the properties of the material. The sensitivity S % increased with increasing operating temperature T. The topmost sensitivity for NO₂ gas was 156 %, with an etching time of 30 s and operating temperature of 200 °C. The faster response speed was 50 s and 75 s at RT for NO₂ gas which was observed at the etching time of 30 s. Therefore, the conclusion from this study is that it is possible to

examine gas sensing properties of different gases like H₂S, CO₂, and volatile solutions like methanol and acetone.

Conflicts of Interest: None.

References:

- Flores-Mendoza MA, Castanedo-Perez R, Torres-Delgado G, Rodríguez-Fragoso P, Mendoza-Alvarez JG, Zelaya-Angel O. Photoluminescence in undoped (CdO) 1- x-(InO₃/2) x thin films at room temperature, 0 ≤ x ≤ 1. *J Lumin.* 2013 Mar 1; 135:133-8.
- Sahu DR, Wu TJ, Wang SC, Huang JL. Electrochromic behavior of NiO film prepared by e-beam evaporation. *Journal of Science: jsamd.* 2017 Jun 1;2(2):225-32.
- Memarian N, Rozati SM, Concina I, Vomiero A. Deposition of nanostructured CdS thin films by thermal evaporation method: effect of substrate temperature. *Materials.* 2017 Jul 9;10(7):773.
- K.N. Abbas, Manal Saleh. "The effect of current density on the structures and photoluminescence of p-type silicon" Third Women scientific conference 7th-8th December .2016 19(1):6269-5.
- Lalithambika KC, Shanthakumari K, Sriram S. optical properties of CdO thin film deposited by chemical bath method. *Int J Chemtech Res.* 2014 Aug 3;6(5):3071-7.
- Sankarasubramanian K, Solaichamy R, Sethuraman K, Rameshbabu R, Ramamurthi K. Structural, optical and electrical studies on CdO thin films using spray pyrolysis technique. *InAIP Conference Proceedings.* 2013 Feb 5; 1512(1): 1036-1037.
- Sarma H, Chakraborty D, Sarma K. X-Ray Analysis of Cadmium Oxide Nanostructured Films Synthesized with Different Precursor Molarities by Silar Method. *Asian J. Chem.* 2017 Sep 1;29(9): 469-73.
- Singh M, Yadav BC, Ranjan A, Kaur M, Gupta SK. Synthesis and characterization of perovskite barium titanate thin film and its application as LPG sensor. *Sens Actuators B Chem* 2017 Mar 31; 241:1170-8.
- Shao Z, Yang X, Zhu G, Zhong M. Photon-induced interfacial charge transfer mechanism of porous silicon/TiO₂ nanoparticles for photoelectrochemical performance. *J Photochem Photobiol a Chem.* 2017 Apr 1; 338:72-84.
- Fan X, Hao Q, Qiu T. Controlled Assembly of Plasmonic Nanostructures Templated by Porous Anodic Alumina Membranes., Springer, Cham. 2015 :249-274.
- Chen L, Schwarzer D, Verma VB, Stevens MJ, Marsili F, Mirin RP, Nam SW, Wodtke. et al., AM.Mid-infrared laser-induced fluorescence with nanosecond time resolution using a superconducting nanowire single-photon detector: New technology for molecular science. *Acc Chem Res.* 2017 Jun 2;50(6):1400-9.
- Wang C, Yin L, Zhang L, Xiang D, Gao R. Metal oxide gas sensors: sensitivity and influencing factors. *Sensors.* 2010 Mar 15;10(3):2088-106.

13. Mou X, Wang J, Meng X, Liu J, Shi L, Sun L. Multifunctional nanoprobe based on upconversion nanoparticles for luminescent sensing and magnetic resonance imaging. *J Lumin.* 2017 Oct 1; 190:16-22.
14. Mizsei J. How can sensitive and selective semiconductor gas sensors be made. *Sens Actuators B Chem.* 1995 Feb 1;23(2-3):173-6.
15. Rahmani MB, Keshmiri SH, Shafiei M, Latham K, Wlodarski W, Du Plessis J, Kalantar-Zadeh K, et al., Transition from n-to p-type of spray pyrolysis deposited Cu doped ZnO thin films for NO₂ sensing. *SENSOR LETT.* 2009 Aug 1;7(4):621-8.
16. Suhail MH, Ibrahim IM, Rao GM. Characterization and gas sensitivity of cadmium oxide thin films prepared by thermal evaporation technique. *Int. J. Thin Film Sci. Tec.* 2012;1(1):1-8.
17. Astruc D, Lu F, Aranzaes JR. Nanoparticles as recyclable catalysts: the frontier between homogeneous and heterogeneous catalysis. *Angew Chem Int Ed.* 2005 Dec 9;44(48):7852-72.
18. Liang YC, Xu NC, Wang CC, Wei DH. Fabrication of Nanosized Island-Like CdO Crystallites-Decorated TiO₂ Rod Nanocomposites via a Combinational Methodology and Their Low-Concentration NO₂ Gas-Sensing Behavior. *Materials.* 2017 Jul 10;10(7):778.
19. Korotcenkov G. Metal oxides for solid-state gas sensors: What determines our choice. *MAT SCI ENG: B.* 2007 Apr 25;139(1):1-23.
20. Akamatsu T, Itoh T, Izu N, Shin W. NO and NO₂ sensing properties of WO₃ and Co₃O₄ based gas sensors. *Sensors.* 2013 Sep 17;13(9):12467-81.
21. Yousif AA, Hasan MH. Gas sensitivity and morphologically characterized of nanostructure CdO doped In₂O₃ films deposited by pulsed laser deposition. *J Biosens Bioelectron.* 2015 Jul 1;6(4):1.
22. L. A. Patil, A. R. Bari, M. D. Shinde, V. V. Deo, and D. P. Amalnerkar, "Synthesis of ZnO nanocrystalline powder from ultrasonic atomization Technique, characterization, and its application in gas sensing," *IEEE Sense.* 2011 Jun 1; 939-946.
23. Al-Jabiry AJ. Studying the effect of molarity on the physical and sensing properties of zinc oxid thin films prepared by spray pyrolysis technique (Doctoral dissertation, Ph. D. thesis, University of Technology).
24. Bai S, Hu J, Li D, Luo R, Chen A, Liu CC. Effect of Calcination Temperature on Sensing Properties for Quantum Size ZnO Crystals. *IEEE Sens J.* 2012 May;12(5):1122-6.
25. Pan LL, Li GY, Lian JS. Structural, optical and electrical properties of cerium and gadolinium doped CdO thin films. *Appl Surf Sci.* 2013 Jun 1; 274:365-70.
26. Fine GF, Cavanagh LM, Afonja A, Binions R. Metal oxide semi-conductor gas sensors in environmental monitoring. *Sensors.* 2010 Jun 1;10(6):5469-502.
27. Akamatsu T, Itoh T, Izu N, Shin W. NO and NO₂ sensing properties of WO₃ and Co₃O₄ based gas sensors. *Sensors.* 2013 Sep 17;13(9):12467-81.
28. Fine GF, Cavanagh LM, Afonja A, Binions R. Metal oxide semi-conductor gas sensors in environmental monitoring. *Sensors.* 2010 Jun 1;10(6):5469-502.
29. Comini E, Baratto C, Concina I, et al., Metal oxide nanoscience and nanotechnology for chemical sensors. *Sens Actuators*
30. Comini E, Baratto C, Concina I, Faglia G, Falasconi M, Ferroni M, Galstyan V, Gobbi E, Ponzoni A, Vomiero A, Zappa D. et al., Metal oxide nanoscience and nanotechnology for chemical sensors. *Sensors and Actuators B: Chemical.* 2013 Mar 31; 179:3-20.
31. Barth S, Hernandez-Ramirez F, Holmes JD, Romano-Rodriguez A. Synthesis and applications of one-dimensional semiconductors. *Progress in Materials Science.* 2010 Aug 1;55(6):563-627 .
32. Kulandaisamy AJ, Reddy JR, Srinivasan P, Babu KJ, Mani GK, Shankar P, Rayappan JB. Room temperature ammonia sensing properties of ZnO thin films grown by spray pyrolysis: Effect of Mg doping. *J Alloys Compd.* 2016 Dec 15; 688:422-9.
33. Kannan S, Rieth L, Solzbacher F. NO_x sensitivity of In₂O₃ thin film layers with and without promoter layers at high temperatures. *Sens Actuators B: Chemical.* 2010 Aug 6;149(1):8-19 .
34. Bai Z, Xie C, Hu M, Zhang S, Zeng D. Effect of humidity on the gas sensing property of the tetrapod-shaped ZnO nanopowder sensor. *Mater Sci Eng.* 2008 Mar 15;149(1):12-7.
35. Yamazoe N, Sakai G, Shimano K. Oxide semiconductor gas sensors. *Catalysis Surveys from Asia.* 2003 Apr 1;7(1):63-75.

تصنيع متحسس غازي ودراسة الخصائص الفيزيائية والمورفولوجي $\text{In}_2\text{O}_3:\text{CdO}$ النانوية لغاز NO_2 للجسيمات

ندى خضير عباس¹

كاظم عبد الواحد عادم²

اشواق طارق دحام¹

¹ قسم الفيزياء، كلية العلوم للبنات، جامعة بغداد، بغداد، العراق.

² قسم الفيزياء، كلية العلوم، جامعة بغداد، بغداد، العراق.

الخلاصة:

تصنيع متحسس غازي ودراسة الخصائص الفيزيائية والمورفولوجي للسليكون المسامي باستخدام عملية الحفر الكهروكيميائية على السليكون باستخدام حامض الهيدروفلوريك المخفف في الماء (1:4) في أوقات حفر مختلفة والتيارات مختلفة. أظهرت فحوصات مجهر القوي الذرية لطوبوغرافية السطح أن متوسط قطر المسام يختلف من 48.63 إلى 72.54 نانومتر مع زيادة وقت الحفر من 5 إلى 15 دقيقة ومن 72.54 إلى 51.37 nm مع زيادة التيار من 10 إلى 30 ملي أمبير.

في حين أظهرت نتائج العينات للتيارات المختلفة أن متوسط قطر المسامية وسماكة طبقة السليكون المسامي انخفض مع زيادة التيار، وجد أن حساسية الغاز من $\text{In}_2\text{O}_3:\text{CdO}$ أشباه الموصلات، لغاز NO_2 ، ترتبط مباشرة بحجم الجسيمات النانوية، وحساسيته يزيد مع زيادة درجة حرارة التشغيل.

الكلمات المفتاحية: المتحسس الغازي، أكاسيد أشباه الموصلات، المورفولوجي، السليكون المسامي.